

PURE BENDING TEST ON A BOX GIRDER WITH LOW PANEL'S SLENDERNESS

José Manuel Gordo

Centre for Marine Technology and Ocean
Engineering (CENTEC), Instituto Superior
Técnico, Universidade de Lisboa
Lisbon, Portugal

Carlos Guedes Soares

Centre for Marine Technology and Ocean
Engineering (CENTEC), Instituto Superior
Técnico, Universidade de Lisboa
Lisbon, Portugal

ABSTRACT

The results of a four points bending test on a box girder are presented. The experiment is part of series of tests with similar configuration but different thickness, spacing between longitudinal stiffeners and span between frames. The present work refers to the stockiest plate box girder with a plate's thickness of 4 mm and a span between frames of 800 mm. The experiment includes initial loading cycles allowing for residual stresses relief. It also includes a series of cycles close to collapse load allowing the analysis of linear characteristic at high levels of load.

The moment curvature relationship is established for a large range of curvatures. The ultimate bending moment of the box is evaluated and compared with the first yield moment and the plastic moment allowing the evaluation of the efficiency of the structure. The post buckling behavior and collapse mode are characterized. Comparison of the experiment with a progressive collapse method is made taking into consideration the effect of residual stresses on envelop of the moment curvature curve of the structure.

INTRODUCTION

The ultimate bending moment that the transverse section of a ship or a floating production and offloading platform (FPSO) can resist under overall longitudinal bending, is one of the main criteria for design of these structures. The move of the industry towards more accurate predictions of the strength of these structures in overall bending to resist still water and wave induced loads requires accurate and expedite methods to assess the ultimate strength.

Caldwell [1] was the first who addressed the plastic collapse of a ship hull under overall bending although he did not allow for buckling of plate elements as pointed out by Faulkner [2]. The first attempt to incorporate the influence of the buckling

collapse of some elements of the cross section was due to Smith [3], who used load shortening curves of individual plate elements to calculate their contribution to the ultimate bending moment of the structure. Other methods based on this general idea were developed including the earlier ones of Billingsley [4], Adamchak [5] and Gordo et al. [6].

Because of their nature, these methods require validation by experimental results. However, the number of test results available in the open literature is still limited. Two box girders representative of bridges were tested by Dowling et al [7] and Nishihara [8] tested seven models of scaled and simplified ship cross sections. An experiment on 1/3 scale model of a frigate was performed by Dow [9], but this was a transversely framed ship which is not representative of most present day structures.

The predictions of the method of Gordo et al [6] reproduced well these tests results [10], but due to the limited extend of geometries involved it was decided to initiate a series of tests that would consider other geometries, covering a wider range of the different parameters that affect the ultimate carrying capacity of such structures under bending. Thus a series of 5 tests on mild steel box girders [11-13] was conducted, where different plate's thickness and frame's spacing were used for the same transverse configuration of the box.

Afterwards tests have been performed on high and very high tensile steel box girders [14, 15] tho allow understanding the influence of the material properties on the ultimate bending moment supported by this type of structure.

In this work the results of a test on a box girder representing the mid-ship region of a ship type structure are presented and analyzed. The specimen is subjected to pure bending leading to a mode of collapse in which the upper flange failed under compressive loads.

EXPERIMENTAL DETAILS

Geometry of the specimen

The specimen is a one-meter long box girder supported by two lateral arms of 2 meters long with much higher rigidity than the box girder. The liaison between them is bolted in order to allow the use of the supports other models.

The four points bending test is sketched in Figure 1 and it allows obtaining pure constant bending throughout the whole specimen.

The central block represents the cross section of a rectangular box girder and has the major dimensions of 1000mm wide and 600mm of depth. The span between the two frames of the specimen is 800mm allowing 100mm in each side for redistribution of stresses.

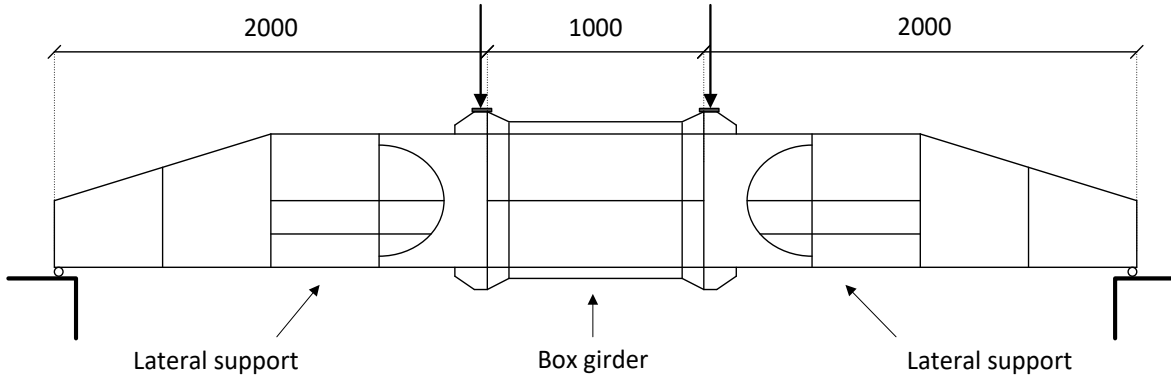


Figure 1 Layout of the experiment and real structure.

The top horizontal and bottom panels have three longitudinal stiffeners equally spaced by 200mm and the lateral webs panels have two stiffeners each, one at the middle and the other half way to the top panel, as presented in Figure 2. This last intermediate stiffener was introduced to reduce the out of plane deformations at collapse in the web panels as result of the collapse of the top panel which induces large deformations in the sides [12, 13].

The nominal plate's thickness is 4 mm with a real average thickness of 4.1 mm and the stiffeners are bars with a thickness of 6 mm and 45mm of depth. This specimen was designated M4-200.

Material Properties

In the design phase of the specimen it was considered that the material to be used would be mild steel with a yield stress (σ_0) of 240 MPa and an elasticity modulus (E) of 210 GPa.

Normal ship building steel shows a marked yield followed by a yielding plateau until 8 to 10 times the yield strain. The hardening is not very marked from this point to the ultimate strain which is normally above 20% of the initial length.

Tension tests were performed in order to obtain realistic values for the material properties and the results obtained show some different values relatively to the initial assumptions.

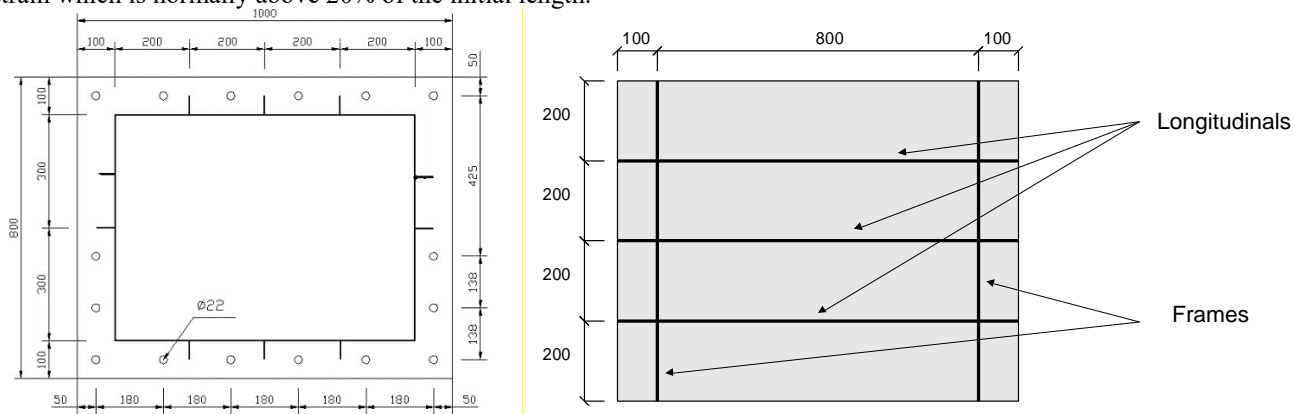


Figure 2 Cross section and stiffeners arrangement

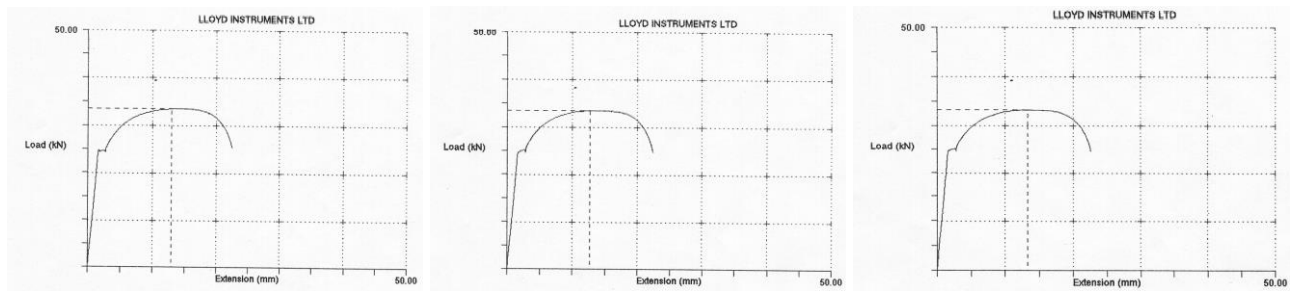


Figure 3 Tensile tests of 4 mm thick plate specimens

Figure 3 shows the output of those tension tests and Table 1 summarizes the main characteristics obtained in the tensile tests with mean values of the yielding stress of 310 MPa and very high ductility.

The stiffeners are 6 mm of thickness and are made of normal steel having a yield stress of 240 MPa. No tensile tests were performed for this thickness.

Table 1. Mechanical properties of 4 mm steel plate used in M4-200 specimen. Tension tests performed by Arsenal do Alfeite, Portugal.

Nominal Dimensions (mm)	Yield stress (MPa)	Maximum stress (MPa)	Maximum Elongation (%)
4.1x19.4	310	420	36.9
4.1x19.5	310	420	37.8
4.1x19.4	310	410	38.0
Média	310	417	37.6

EXPERIMENTAL RESULTS

The experiment was conducted in several cycles of loading followed by total discharges. This procedure was adopted due to

the existence of residual stresses in the specimen. During the initial loading cycles, the residual stresses in the panel under tension were reduced to low values. Thus its effect on the early stage of loading is removed and the initial structural modulus (EI) may be obtained from the experiment and compared with the calculated value.

Vertical load-displacement curve

Figure 4 shows the relationship between the vertical load and global vertical displacement obtained in all cycles of loading. The maximum vertical load supported by the box was 609 kN at a vertical displacement of 61.7 mm. After this displacement the structure was further loaded by 10% to characterize the post collapse behavior.

The first cycle reached the maximum load of 122 kN with an imposed displacement of 8.5 mm. This load level is approximately 10% of the first yielding load in elastic domain which is 945 kN. After this cycle one has a residual displacement of 1.3 mm.

More detail analysis of the first cycle, as shown in Figure 5, allows one to conclude that there is not much residual stress relief due to cycling loading until the reversal load at 122 kN since the energy absorbed, given by area within the cycle line, is low in comparison to the elastic energy, and approximately half

of that energy is due to structural hysteresis. In fact, the difference in average between the loading path of the first cycle and the loading path of the second is only 0.37 mm apart. It corresponds to a total dissipation of energy of 44.6 J due to residual stresses relief and of 34.7 J due to structural hysteresis. The potential elastic energy computed at displacement of 8.52mm in the second cycle was 345 J, ten times more than the structural hysteresis energy.

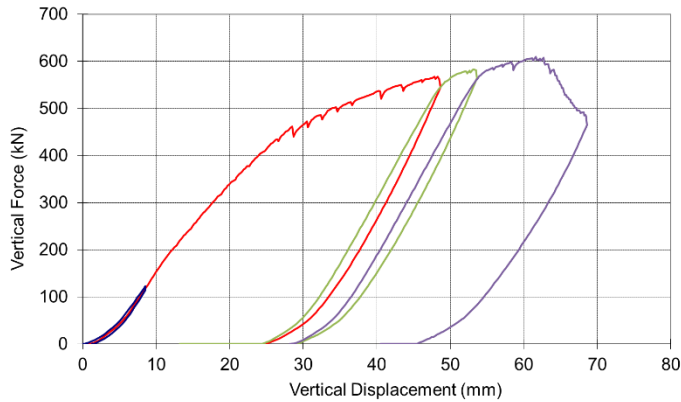


Figure 4 - Vertical load-vertical displacement curves for all cycles of loading

It also may be noted a 6% shedding of load at reversal with a constant displacement of 8.5 mm which is observed in others similar experiments [15].

The second and third cycles have achieved a maximum load below the ultimate load and the loading paths are strongly non-linear after being reached the previous maximum.

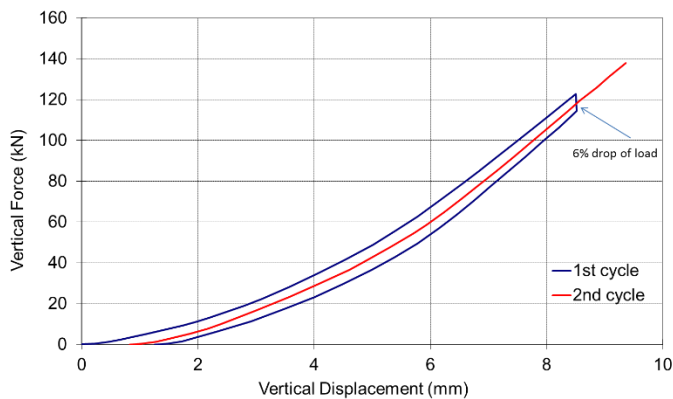


Figure 5 First cycle and initial phase of second cycle

The second cycle presents three different behaviors. The initial one is given by the dashed line in Figure 6, and represents the linear behavior until the maximum load of cycle 1. The three dashed lines are parallel and indicate the linear relation between load and displacement after residual stress relief. Softening below 100 kN in all cycles are result of the contact between the flanges of the box and the supports to be bolted and not welded.

The second stage, indicated by line A, initiates approximately at 250 kN until 400 kN and is due to the reduction in the effective moment of inertia by premature plasticity in the welding of the bottom panel that is in tension [16].

The third and last stage (line B) is similar in terms of rigidity to the third and fourth cycles until the collapse. This additional reduction on the slope of the moment-curvature curve of the structure is a result of the effect of residual stress in the whole box-girder and the development of collapse deformed shape at this level of load. However, the ineffectiveness due to residual stresses in tension and compression seems to be more important than the magnification of the out of plane deformations due to the fact that the slope is almost constant.

It should be noted that the local shedding of load in intermediate curvatures is result of stopping the experiment which conducted to decrease of the net load and a slight increase in the vertical displacement. This is common in hydraulic flow control of the experiment and its magnitude depends on the speed of loading and the degree of plasticity that is occurring in the structure at that load [15].

The energy dissipated in this second cycle is very large. The area inside load-displacement curve of the second cycle computes 16.9 kJ and the dissipation of energy by plasticity due to residual stresses relief is 11.3 kJ, as presented in Table 2.

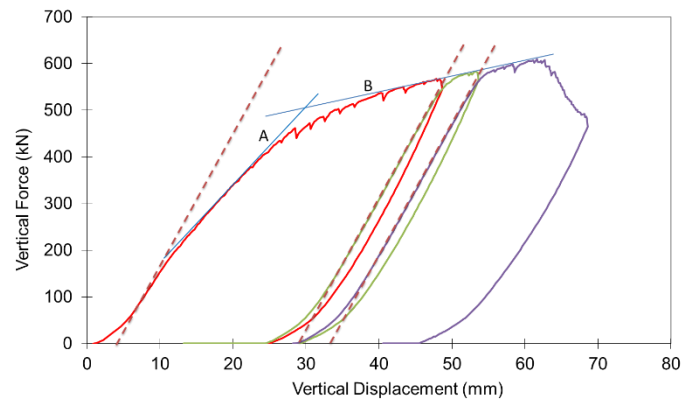


Figure 6 Different stages on the structural behaviour of the box-girder

It should be noted that this dissipation of energy includes the energy dissipated in the central span of the box girder where the stiffeners and the plating are welded by intermittent alternate welding but also and especially by the plasticity of the heavily welded two strips of 100 mm in each side of the box girder connecting to the external flanges.

The third cycle confirms a linear relationship between vertical load and vertical displacement until the equilibrium at reversal of previous cycle and, after that, the evolving line B is regained to the same rigidity observed in the end of loading of the second cycle.

Figure 7 shows the deformations on the top panel in compression at intermediate load level on third cycle after suffering the stress relief on the second cycle. It does not present

any relevant out of plane deformations in plating or stiffeners apart a slight 3 wave shape in the nearest plate and an upward one wave shape in the two central plates of low magnitude.

At collapse stage, the top panel presents a global upward deflection on the stiffeners and 4 to 5 half-wave shapes in the plating, as shown in Figure 8. Also at this stage one of the welded connections in the bottom panel has failed, Figure 9, but this failure is not reflected in the load-displacement curve since the continuity was ensured by the plating. However, the same is not

applicable in respect to the moment-curvature relationship since the curvatures are measure in the end of the supporting structure and an apparent magnification of the measured curvature is expected due to this failure.

The fourth cycle imposed a vertical displacement that conducts the box girder through collapse and beyond. The maximum vertical load was 609.2 kN at a displacement of 61.7 mm followed by a deep and continuous reduction of load.

Table 2 Energy balance

Cycle	Data		Energy (kJ)					Ratio
	Displacement (mm)	Load (kN)	Maximum	Total	Previous Maximum	Residual Stress	Structural Hysteresis	SH/Load (J/kN)
1	8.5	114.5	0.39	0.08		0.045	0.035	0.30
2	48.6	545.2	16.94	12.00	0.35	11.34	0.658	1.20
3	53.6	564.4	8.44	3.15	5.60	2.44	0.702	1.24
4	61.7	609.2	10.71	10.43	6.00			

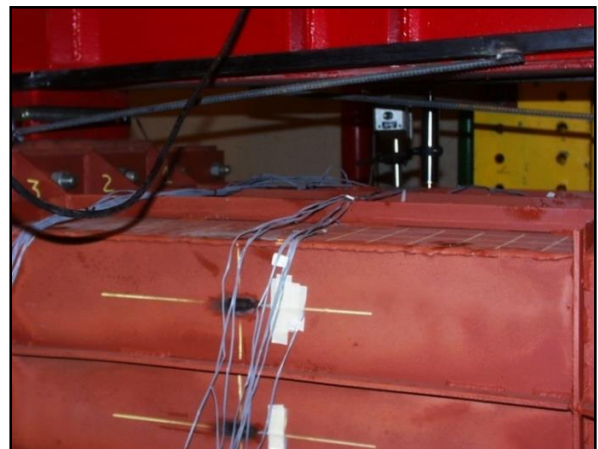


Figure 7 View of top panel at intermediate load on 3rd cycle from opposite sides

Figure 8 - Collapse's stage: magnification of out of plane deformations on the top panel under compression



Figure 9 Welding failure in bottom bracket connection at collapse stage

Relationship between the moment and the curvature

The bending moment is calculated directly from the product of the applied force and the distance from the lateral support to the nearest point of loading; the change in horizontal distance is negligible due to the small angle during loading. The curvature was calculated by gauges' measurements in two similar auxiliary devices located in each side of the box which measure the deflection angle of rotation between the two connecting sections to the supporting structures. The moment curvature curve is presented in Figure 10.

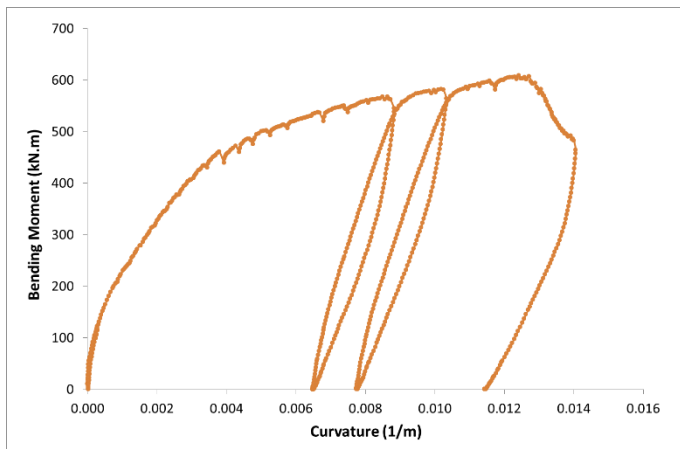


Figure 10 Moment-curvature relationship for complete test

In this test one of gauges stopped temporarily to provide relevant information so the analysis of the results is based on measurements of the other gauge instead of being based on the average of the two. However, the correlation between the two gauges is quite good in the range where both measurements were available, except for very low loads by the difficulty of having full contact between the flanges of the connections at low loads and the gauges for curvature assessment are measuring the displacements on the end of the supporting structures. Due to this

fact the discussion of results is limited to the range above 200 kNm.

The envelope of moment-curvature curves shows the same characteristics of the vertical load-displacement curve, i.e., a first constant rigidity in the second cycle from 200 to 400 kNm and a second phase until collapse, involving global residual stresses effects and deformations due to high level of load.

The first cycle results are highly conditioned by a transverse rotation of the girder which corresponds in fact to a twist until 80 kNm from which the dependence between the two transducers that reads the curvature becomes linear and unitary. At the end of the first cycle residual curvatures are generated which also corresponds to a slight residual permanent transversal rotation which may be result of the asymmetry residual stresses pattern in the top and bottom panel.

Figure 11 shows the load cycles to which the structure is subjected having removed the residual curvature existing at the beginning of each cycle.

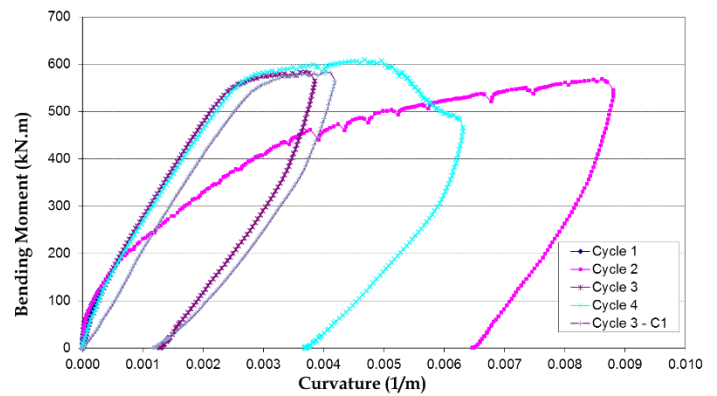


Figure 11 - Bending moment-curvature relationship with previous residual curvature removed

The coincidence of the quasi-linear part of the curves of the third and fourth cycles shows that after having loaded the structure to certain levels where global elastic-plastic phenomena overlap particular aspects related to residual stresses and initial deformations, no longer makes sense to consider the effect of residual stresses because they were relieved. There is, however, a small increase of rigidity from the third cycle to the fourth, because the third cycle will generate bigger permanent deformations to those it has started, that is, 'initial imperfections' of the fourth cycle are higher than the ones of the third despite having similar shape of out of plane deformations which was fixed by plastic deformation in the first cycles. These higher 'defects' make the three-dimensional structure become slightly more flexible.

In the same figure it is also presented the curve obtained using the information from the other gauge installed to measure the curvature (C1).

The parallelism between the two curves for the third cycle constructed with data from different gauges, shows that beyond a bending moment higher than 150 kNm to which the box has a

transverse rotation due to some asymmetry, this twist ceases to be important and can be ignored.

If instead one considers the absolute curvature from the beginning of the test, Figure 10, it is found that:

1. the curvature at collapse obtained for this thicker model is quite high in comparison with those found in slender box girders with similar geometry [12, 13];
2. hysteresis is very pronounced and dissipates energy;
3. the discharge does not affect much the subsequent loading of the structure beyond the previous maximum, since the mode of deformation is stabilized;
4. the post collapse region presents a rather sharp unloading;
5. the residual curvature after collapse is very high.

A peculiar aspect on the discharge of load in all cycles is the existence of three different regions in terms of rigidity, measured by the slope of the curve: the first is the initial discharge and has a slope higher than the slope of the load in elastic range until approximately 350 kNm; the second stage from 350 to 150 kNm has a structural modulus similar to the elastic modulus; and the total discharge presents values of the modulus less than the elastic modulus. In fact, these different regions are responsible for the structural hysteresis of the box under cycling bending moment, as presented in Table 2 by the energy dissipated.

Structural Modulus

The effective structural modulus is the slope of the relationship between the bending moment, M , and the curvature, φ , at any point of load and may be represented by the product of the modulus of elasticity of material, E , and the effective moment of inertia of the cross section, I_e at a certain load level. For a perfect structure in elastic range, the whole cross sectional area is fully effective and the effective moment of inertia is the second moment of area, I , which is equal to 10.25 dm⁴ for this box and a structural modulus of 215 MNm². The relation is given by:

$$\frac{dM}{d\varphi} = EI_e = k_c EI \quad (1)$$

The effectiveness factor, k_c , depends mainly on residual stresses, initial imperfections, load level and geometrical uniformity along the structure.

Estimates for the tangent structural modulus were performed as function of the curvature imposed on every cycle, having separate load and unloading phases. Also the tangent modulus was evaluated in the post collapse region, as presented in Figure 12.

Structural tangent modulus during loading

The structural modulus during loading allows to distinguish two very different types of cycles. The cycle 2, where the residual stresses and their relief is an important form of energy dissipation, features the elastic-plastic nature of the moment-curvature curve, making the tangent modulus to present reduced values and a decreasing trend. The third and final cycles have similar behavior in terms of the curvature on the initial elastic stage of each cycle, allowing an overlap almost perfect of the two curves. However, it also confirms that the structural modulus in

the elastic region is marginally less on the final cycle in comparison to the third one, as stated before. This is result of the increase in the permanent out-of-plane deformations due to elastic-plastic deformations in the 3rd cycle.

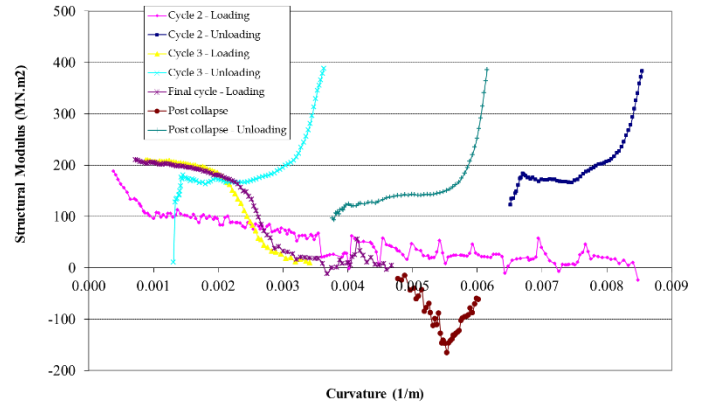


Figure 12 - Tangent structural modulus versus curvature calculated from M4-200 experiment

Two very different regions can be clearly identified in the second group when the structural modulus is presented against the bending moment, Figure 13. The first zone is almost constant at a plateau modulus around 200 MNm² corresponding to the theoretical structural modulus of the box that is 192 MNm², after the partial relief of residual stresses and showing an almost linear elastic behavior. The other zone presents a drastic reduction in tangent modulus after reaching the maximum point in the previous cycle, directly related to the elastic-plastic regime associated with progressive development of the buckled deformed shape and fixing it by permanent plastic deformation in both plating and stiffeners.

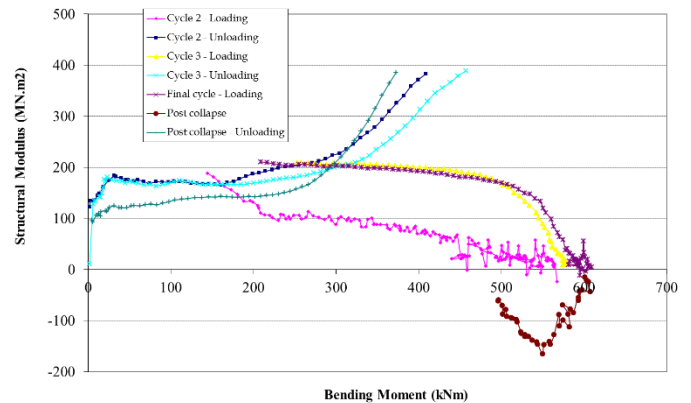


Figure 13 Tangent structural modulus versus bending moment calculated from M4-200 experiment

It is this definitive adjustment of the deformed shape of the panels of the box that characterizes the first cycles where the relief of residual stresses by plastic deformation are very important. It may also be identified the loading point of the second cycle when the connection bracket broke, as shown in Figure 9. This leads to sudden reduction on the structural

modulus at 450 MNm^2 , followed by a redistribution of stresses and a recovery of the previous trend due to this new equilibrium.

Structural tangent modulus during unloading

The dependence of the tangent modulus to curvature in discharge is similar on all cycles and one can identify two regions: one, immediately after having imposed the maximum curvature, with very high values and exceeding largely the elastic modulus, which decays rapidly to a level between 170 and 180 MNm^2 with decreasing curvature, i.e. approximately 85% of the elastic modulus. The second phase is a plateau at this level for a bending moment below 200 kN.m .

In Figure 14, the abscissa is changed by subtracting the current curvature from the maximum curvature reached on each cycle. It can be seen that the modulus of the cycles prior to the collapse's cycle overlap almost perfectly, while the magnitude of the discharge after the collapse cycle follows the initial trend of the others cycles, but the plateau is reached at lower values of the modulus due to the very low stiffness of the deformed structure, as it is presented in the Figure 15 at the end of the test.

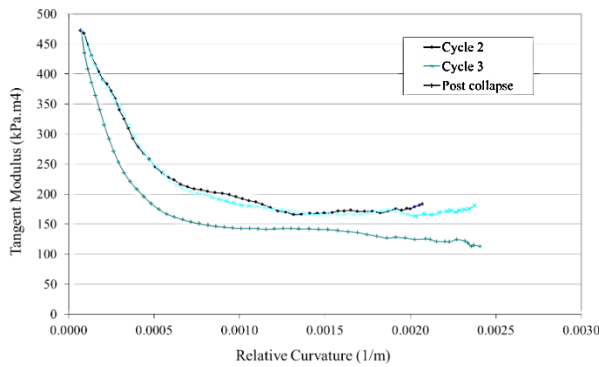


Figure 14 Tangent modulus at unloading versus the relative curvature to maximum curvature

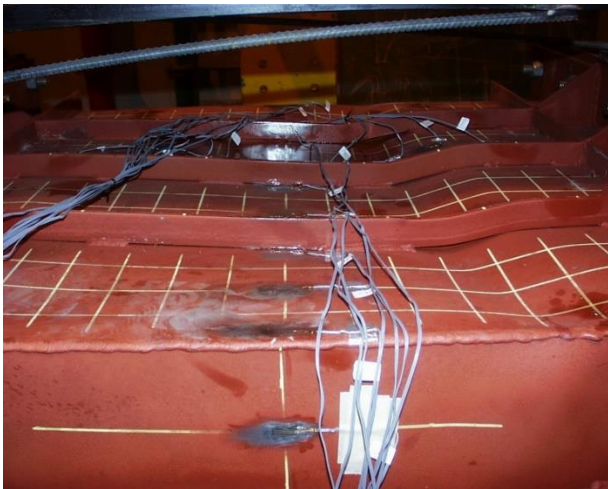


Figure 15 Shape of top panel under compression after collapse and total discharge

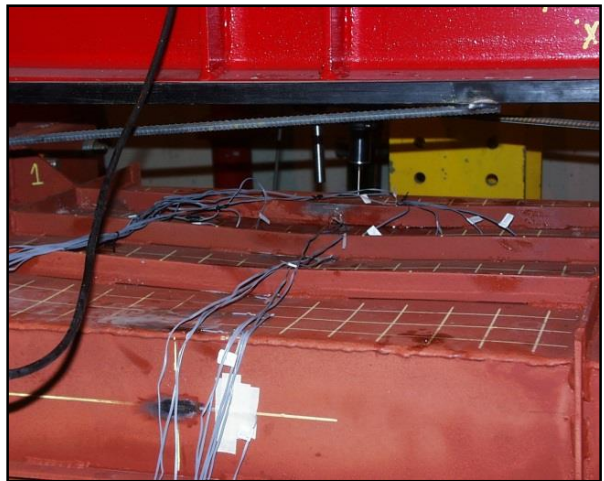


Figure 16 Deformations at collapse (top) and at the end of test (bottom).

Tangent modulus in post-collapse regime

The behavior after collapse is characterized by having a negative tangent modulus. In the analysis of the behavior of a structure it becomes important from the point of view of strength not only to know the ultimate bending moment but also to know if the collapse occurs abruptly or smoothly. This last feature can be set through the tangent modulus.

Figure 14 depicts the variation of the tangent modulus to the curvature and it notes that the maximum modulus at this stage (-165 MNm^2) takes values of the order of magnitude of the tangent modulus at elastic regime under loading with deformations well developed and stabilized.

This means that this box, despite being constructed with panels of intermediate slenderness has a very rapid discharge for curvatures beyond the collapse's curvature. This phase should correspond to developing large plastic deformations in the ribs, as shown by the large vertical deformation of the reinforcements in Figure 15. It follows a deformation phase more or less stabilized in which the tangent modulus returns to substantial smaller negative values.

It is interesting to note that the geometric deformations at collapse presented in the top of Figure 16 are rather different than those presented at the end of test, after a deep loading in post-collapse, as shown in the bottom of the same figure.

EFFECT OF SLENDERNESS ON ULTIMATE BENDING MOMENT

The present test result is now compared with 5 similar tests performed on mild steel box-girders with identical geometry.

Two of them belong to the same series and they are thinner, respectively 3 and 2 mm plate's thickness [11-13]; the other 3 belong to a different series with more than one frame' span and small stiffener' spacing (150mm) but with similar cross section arrangement [14, 15].

Table 3 presents the geometrical properties of the box-girder and the mechanical characteristics of the material.

The results of the tests are presented in Table 4 where it is calculated the structural efficiency (SE) given by ratio between the ultimate bending moment (UBM) and the first yield bending moment (YBM) and the ratio between the UBM and the structural modulus (EI) or a measure of the section modulus assumed as EI/D for objectivity. D is the nominal height of the box-girder.

Figure 17 presents the relationship between the UBM/EI and the plate slenderness β . This ratio (UBM/EI) is typically a unitary bending moment in relation to the geometry of the cross-section in terms of dimensions and thicknesses and should be a measure to compare different types of box-girders and ships made of different materials.

Table 3 Geometric and material properties of box-girders

	M4-200	M3-200	M2-200	N200	N300	N400
a (mm)	800	800	800	200	300	400
t (mm)	4.1	3	2	4	4	4
b (mm)	200	200	200	150	150	150
b/t	48.8	66.7	100.0	37.5	37.5	37.5
S _{yp} (MPa)	310	183	177	270	270	270
S _{yst} (MPa)	240	310	183	270	270	270
E (GPa)	210	210	210	200	200	200
I (dm ⁴)	8.33	6.86	4.13	7.68	7.68	7.68
A _b (dm ²)	1.13	0.98	0.63	1.21	1.21	1.21
R (mm)	272	264	256	252	252	252
2R/D	0.91	0.88	0.85	0.84	0.84	0.84
h (mm)	45	45	30	200	200	200
tw (mm)	6	4	3	4	4	4
A _t (mm ²)	1090	780	490	680	680	680
A _p (mm ²)	820	600	400	600	600	600
A _s (mm ²)	270	180	90	80	80	80
r (mm)	8.6	8.6	8.6	7.6	7.6	7.6
a/r	93.02	93.02	93.02	26	40	53
β	1.87	1.97	2.90	1.38	1.38	1.38
λ	2.98	2.17	3.05	0.97	1.46	1.94

Figure 18 plots the dependency of the same quality in relation to the column slenderness. Here the effect is more

marked and, at least according to these data, more important than the effect of the plate slenderness.

Table 4 Test results and evaluation of main parameters

	M4-200	M3-200	M2-200	N200	N300	N400
EI (MNm ²)	215	151	87	153.6	153.6	153.6
Yield Moment (kNm)	890	419	244	669	669	669
Ultimate Moment (kNm)	609	349	173	643	512	475
SE - Structural Efficiency	0.68	0.83	0.71	0.96	0.77	0.71
UBM/EI (1/(1000.m))	2.83	2.31	1.99	4.19	3.33	3.09
UBM*D/EI (1/(1000))	1.70	1.39	1.20	2.51	2.00	1.86

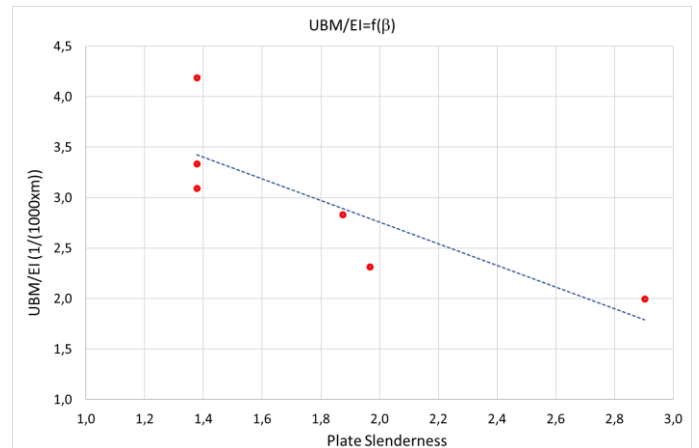


Figure 17 Effect of plate slenderness on UBM/EI

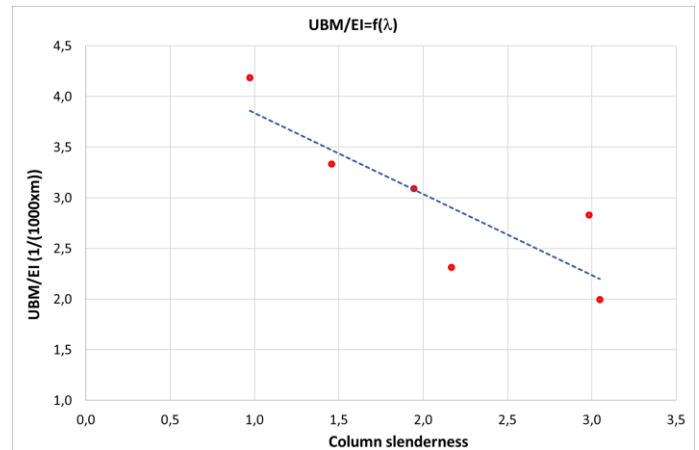


Figure 18 Effect of column slenderness on UBM/EI

A trial has been made to compute the effect of both parameters together, simply by multiplying them. The results are plotted in Figure 19. The dependency is almost linear and the inverse of the product of both plate and column slenderness is considered. The UBM may be expressed as:

$$UBM = \left(\frac{3.13}{\beta\lambda} + 1.84 \right) EI \cdot 10^{-3} \quad (2)$$

Finally, it should be said that the ratio UBM/(EI/D) should be more representative for futures analyses where different geometries are compared but it was no effect on this data since D is the same for all boxes. It results for this data in:

$$UBM = \left(\frac{1.88}{\beta\lambda} + 1.10 \right) \frac{EI}{D} \cdot 10^{-3} \quad (3)$$

Both formula uses IS unit system.

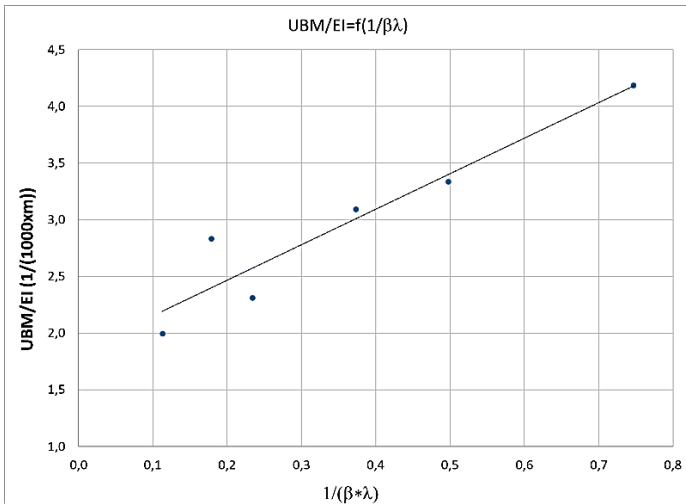


Figure 19 Effect of slendernesses on UBM/EI

CONCLUSIONS

The result of a four bending test on a box girder is presented including the analysis of several cycles of loading in relation the moment-curvature curves, dissipation of energy by residual stresses relief and hysteresis, and variation of structural modulus with loading.

Emphasis is given for the comparison of the test with similar ones and, from the analysis, it may be concluded that the ultimate bending moment depends on the structural modulus of the cross-section, the plate and column slenderness.

A linear dependency is found when the inverse of the product of the slendernesses is used which allows to derive an expression that includes the main contribution for the ultimate bending moment of metallic structures. It includes the geometry of the cross-section I, the particulars of the stiffened plates in compression on β and λ , the mechanical properties of the materials, respectively the Young Modulus E and the yield stress S_y indirectly in β and λ . The scatter of the data increases when the product of the slendernesses increases above 3.

ACKNOWLEDGEMENTS

The experimental work has been performed in the scope of the project MARSTRUCT, Network of Excellence on Marine Structures (<http://www.mar.ist.utl.pt/marstruct/>), which has been financed by the EU through the GROWTH Programme under contract TNE3-CT-2003-506141. This paper was completed in the scope the project "Ship Lifecycle Software Solutions", (SHIPLYS), which was partially financed by the European Union through the Contract No 690770 - SHIPLYS - H2020-MG-2014-2015.

REFERENCES

- [1] J.B. Caldwell, Ultimate longitudinal strength, *Transactions of RINA*, 107 (1965) 411-430.
- [2] D. Faulkner, contribution to the discussion of "Ultimate longitudinal strength" by J. Caldwell, *Transactions of RINA*, 107 (1965).
- [3] C.S. Smith, Influence of local compressive failure on ultimate longitudinal strength of a ship's hull, in: *3th Int. Symposium on Practical Design in Shipbuilding*, Tokyo, 1977, pp. 73-79.
- [4] D.W. Billingsley, Hull girder response to extreme bending moments, in: *5th STAR Symposium*, SNAME, 1980, pp. 51-63.
- [5] J.C. Adamchak, An approximate method for estimating the collapse of a ship's hull in preliminary design, in: *Ship Structures Symposium '84*, 1984, pp. 37-61.
- [6] J.M. Gordo, C. Guedes Soares, D. Faulkner, Approximate assessment of the ultimate longitudinal strength of the hull girder, *J Ship Res*, 40 (1996) 60-69.
- [7] P.J. Dowling, S. Chatterjee, P. Frieze, F.M. Moolani, Experimental and predicted collapse behaviour of rectangular steel box girders, in: *International Conference on Steel Box Girder Bridges*, London, 1973.
- [8] S. Nishihara, Ultimate longitudinal strength of mid-ship cross section., *Naval Arch. & Ocean Engng.*, 22 (1984) 200-214.
- [9] R. Dow, Testing and analysis of a 1/3-scale welded steel frigate model, in: R.S.D.a.C.S. Smith (Ed.) *Advances in Marine Structures 2*, 1991, pp. 749-773.
- [10] J.M. Gordo, C. Guedes Soares, Approximate method to evaluate the hull girder collapse strength, *Mar Struct*, 9 (1996) 449-470.
- [11] J.M. Gordo, *Ultimate Strength of Ship's Structures under Bending Moment* in, Instituto Superior Técnico, Technical University of Lisbon, Portugal, 2002, pp. 450.
- [12] J.M. Gordo, C. Guedes Soares, Experimental Evaluation of the Ultimate Bending Moment of a Box Girder, *Marine Systems and Offshore Tecnology*, 1 (2004) 33-46.
- [13] J.M. Gordo, C. Guedes Soares, Experimental evaluation of the ultimate bending moment of a thin box girder, in: *33rd International Conference on Ocean, Offshore and Arctic Engineering OMAE 2014*, ASME, San Francisco, 2014.
- [14] J.M. Gordo, C. Guedes Soares, Tests on ultimate strength of hull box girders made of high tensile steel, *Mar Struct*, 22 (2009) 770-790.
- [15] J.M. Gordo, C. Guedes Soares, Experiments on three mild steel box girders of different spans under pure bending moment, in: C.G. Soares, J. Romanoff (Eds.) *Analysis and Design of Marine Structures*, Taylor & Francis, 2013, pp. 337-346.
- [16] J.M. Gordo, Residual stresses relaxation of welded structures under alternate loading, in: *Developments in Maritime Transportation and Exploitation of Sea Resources*, Taylor & Francis, 2014, pp. 321-328.